diffusion-fundamentals.org

The Open-Access Journal for the Basic Principles of Diffusion Theory, Experiment and Application

Recent Progress in the Simulation of Diffusion Associated with Hollow and Bi-Metallic Nanoparticles

Graeme E. Murch[1], *Alexander V. Evteev*[1], *Elena V. Levchenko*[1] *and Irina V. Belova*[1]

[1]University Centre for Mass and Thermal Transport in Engineering Materials
Priority Research Centre for Geotechnical and Materials Modelling
School of Engineering
The University of Newcastle

Corresponding author:
Prof. Graeme E. Murch
School of Engineering
The University of Newcastle
Callaghan, New South Wales 2308, Australia
E-Mail: Graeme.Murch@newcastle.edu.au

Abstract

In this paper, we review the recent understanding gained by kinetic Monte Carlo and molecular dynamics simulation and related theory of the diffusion processes involved in 1) the formation and later shrinkage of hollow nanoparticles and 2) the formation of segregated bi-metallic nanoparticles.

Keywords: Nanoparticles, Kirkendall effect, diffusion, molecular dynamics, Monte Carlo, segregation

1. Introduction

The potential for employing atomic diffusion to 'self-assemble' nanoparticles having tailored spatial distributions of the components has been recognized in recent years but gaining an understanding of the underlying processes is still in its relatively early stages. Much of the understanding is coming from computer simulations, using the methods of molecular dynamics and kinetic Monte Carlo. In the present paper, we review some of the progress that has been made using computer simulation and related theory in understanding the formation and shrinkage of hollow nanospheres and the formation of segregation bi-metallic nanoparticles.

Hollow Nanospheres (background)

The synthesis of hollow nanospheres with tailored void sizes is of great interest because of the wide range of possible industrial applications of such nanoparticles. Applications include vehicles for precise medication delivery, nano-chemical reactors for the precise control of catalytic reactions in the petrochemical industry, containers of environmentally sensitive species, components of ultra-lightweight structural materials and many others. Yin *et al.* [1] were the first to demonstrate that the Kirkendall effect

© 2009, G. E. Murch

(with Kirkendall porosity) [2], a phenomenon well-known in interdiffusion processes in metallic alloys, can be utilized at the nano-level to form uniform hollow nanospheres of *CdS, CdSe, CoO, CoSe,* Co_3S_4, Co_9S_8. The general strategy is to start with the faster diffusing component as the core and surround it with a slower diffusing component. Upon interdiffusion, in the absence of conventional vacancy sinks, the net flux of vacancies into the material leads to a central void. Yin and colleagues' finding has encouraged many subsequent studies which have included, for example, the formation of hollow nanospheres of Fe_3O_4/Fe_2O_3 [3], Y_2O_3 [4], Cu_2O [5], *ZnO* [6], *NiO* [7] and Li_2NH [8] as well as nanotubes of Ag_2Se [9], $CoSe_2$ [10], *CdS* [11], $ZnAl_2O_4$ [12]. In principle, the structure and properties of hollow nanoparticles can be tuned by varying the starting composition, size and shape, but this will only be possible once a thorough understanding of the phenomenon has been gained.

It is interesting to note that the formation of hollow micro-sized crystals by the Kirkendall effect was first demonstrated some thirty five years ago: Aldinger [13] obtained shells of a *Be-Ni* alloy after annealing *Be* microparticles of 33 μm diameter that had been coated with *Ni*. Similar findings were also reported in the Soviet literature of the time [14]. Alternative methods of synthesis of hollow nanoparticles, mainly using various template strategies, have been identified including a method to form hollow nanoparticles of noble metals [14]. In general, such methods do not make direct use of atomic diffusion.

Hollow nanoparticles can be expected to be unstable with respect to shrinkage via diffusion to a solid nanoparticle in order to reduce the total surface area. This has recently been demonstrated experimentally [5]. The possibility of shrinkage and the resulting loss of longevity mean that the stability of hollow nanoparticles and the shrinkage process needs to be thoroughly understood too.

Bi-metallic Nanoparticles (background)

In general, at the nanoscale, bimetallic particles can form various kinds of structure, ranging from the high entropy situation such as a random solid solution to the low entropy structure such as a layered compound or core-shell structure. Segregation of a component such as a noble metal can be superimposed on this. In principle, the structure and properties of bimetallic nanoparticles can be tuned by varying such parameters as composition, size, shape and surface energy. All of these make use of diffusion.

It is well-known that *Ag* and *Pd* are metals with important existing and potential applications as catalysts. With their very high surface areas, *Ag* and *Pd* nanoparticles are especially efficient, but there are still substantial negative economic aspects because of their high cost. Since catalytic reactions occur at the surface, a large fraction of metal in the core of the nanoparticle is in fact effectively wasted. Bimetallic nanoparticles are currently attracting a great deal of interest due to their unique physical and chemical properties [15]. An interesting bimetallic nanoparticle combines *Ag* or *Pd* with a lower cost and higher surface energy metal such as *Ni* [16-22]. It would of course then be economically attractive for the precious and catalytically active *Ag* or *Pd* atoms to be allowed to segregate (by diffusion) to the surface to reduce the overall surface energy.

In both cases of hollow nanoparticles and bimetallic nanoparticles, the search for compositions, sizes, shapes and technological ways for fabricating them to exhibit desirable structures and properties is a highly complex problem that requires a deep physical understanding of the diffusion processes and the local stability of structures that occur at the nanoscale. In the following sections, we will discuss the formation (and shrinkage) of hollow nanospheres. This will be followed by a discussion of the formation of (segregated) bimetallic nanospheres.

2. Formation of Hollow Nanospheres

In general terms, the formation of hollow nanoparticles is simply a natural result of the phenomenon of Kirkendall porosity coming by way of the Kirkendall Effect. During interdiffusion of a bulk diffusion couple, say of two pure metals, the fluxes of the two opposing atomic components will in general not be equal. As a result, there will be a net flux of vacancies from the slow diffuser side to the fast diffuser side. This is known as the Kirkendall Effect and was the outcome of the famous experiment in the late 1940s that proved conclusively that vacancies were the principal vehicles for diffusion in metals [2].

In an 'ideal' interdiffusion situation, vacancies are maintained at equilibrium everywhere in the diffusion zone: vacancies are created and annihilated as locally required 1) by the process of dislocation climb and/or 2) at grain boundaries and/or 3) at free surfaces. This requires of course that such vacancy sources and sinks are sufficiently numerous and efficient for this purpose. However, on the faster diffuser side, the usual sinks for vacancies mentioned above may be unable to cope with the influx of vacancies, especially when the diffusion rates of the two atomic species are very different. On this side, vacancies above the saturation concentration then start to aggregate into pores. In effect, the vacancies are forming their own sinks. Pores formed in this way are collectively referred to as Kirkendall porosity. Over time, these pores can eventually join together to form large voids. In the joining technology that depends on diffusion-bonding, the phenomenon of Kirkendall porosity has generally been viewed as a significant nuisance because of the considerable loss of mechanical strength at the bond that can ensue.

At the nano-scale, the small distances involved in the interdiffusion process and the absence of many conventional vacancy sinks such as dislocations has meant that Kirkendall porosity can become especially prominent and, in fact, presents a valuable method for fabricating hollow nanostructures. The recent demonstration by Yin and co-workers [1] of the formation of a very large void in the centre of an initially solid nanosphere, thus creating a hollow nanosphere, attracted widespread interest because of the significant potential for new technological applications as mentioned above.

Several papers appeared in 2005 that provided the formal beginning of a theory of formation of a hollow nanosphere. We will briefly describe them here. Tu and Gösele [23] considered the role of the Gibbs-Thomson potential on the rate of change of radius r of the nanosphere to obtain:

$$\frac{dr}{dt} \approx \frac{D_A}{kT}\left(-\frac{\Delta\mu}{r_{II} - r_I}\right) \tag{1}$$

where

$$\Delta\mu = \Delta G_f + 2\Omega\left(\frac{\gamma_{II}}{r_{II}} + \frac{\gamma_I}{r_I}\right)$$

and ΔG_f is the free energy of formation of the product phase, γ_I, γ_{II} are the interfacial energies at inner and outer surfaces *I* and *II*. Ω is the atomic volume, D_A is the diffusivity of the faster moving component and k and T are the Boltzmann constant and absolute temperature respectively. Since the interfacial energies are not generally known, the growth rate cannot be determined from Eq. 1. Within limits, the driving force will probably not change much in the nano-scale. In principle, for very high values of γ and small values of r, the Gibbs-Thomson potential may be positive, potentially preventing out-diffusion of the high mobility component and therefore preventing the formation of a hollow nanosphere.

Starting with the Onsager formalism of irreversible thermodynamics, Belova and Murch [24] sketched an alloy interdiffusion theory for the general case of interdiffusion of two completely miscible metals A and B to form an isomorphous alloy but where there are no implied sources and sinks of vacancies. This contrasts with the conventional treatment of bulk interdiffusion of two miscible metals where the vacancies are assumed to be always at equilibrium [25]. This model would correspond to the formation of a shell of an alloy AB starting from a core of metal A (of high mobility) surrounded by a shell of metal B (of low mobility). Expressions were developed for the fluxes of the components in the Manning random alloy model diffusion kinetics approximation [26]. Moving boundary kinetic Monte Carlo simulations of interdiffusion for such a model in a constant gradient of vacancies verified the expressions. The simulations showed that in principle, at very late times, after the formation of a homogeneous alloy shell, any continued flux of vacancies should then produce some segregation of the atomic components. This phenomenon is sometimes referred to as the Inverse Kirkendall Effect and is known to occur in the net flux of vacancies occurring during radiation damage annealing of alloys.

Prasad and Paul [27] addressed the rate of appearance of a phase β from an inner phase α (A-rich) and an outer phase γ (B-rich) for the geometry of a nanorod. At the interface *I* (between α and β) and identified by the radius r_I, A will be dissociated from the α phase to produce the β phase. Dissociated A will also diffuse through the β phase to react with the γ phase to produce more β phase at the *II* interface (identified by r_{II}). The β phase thus grows from both interfaces *I* and *II*. Using Wagner's suggestion of an integrated diffusion coefficient of a 'line compound' Prasad and Paul showed that for a pure element core and shell an integrated diffusion coefficient of the β phase can be written as:

$$\widetilde{D}^{\beta}_{\text{int}} = \frac{(r_{II} - r_I)N_B^{\beta}\left(1 - N_B^{\beta}\right)\Delta A_r^{I/II}}{4\pi t(r_0 - r_I)} = N_B^{\beta}\left(1 - N_B^{\beta}\right)k_g \qquad (2)$$

where $\Delta A_r^{I/II}$ is the area between interfaces *I* and *II*, N_B^{β} is the average composition of the β phase and k_g is a growth constant. The growth rate of the product phase and the consumption rate of shell and core should follow parabolic kinetics and could in principle be determined**.** When vacancies are at equilibrium during the interdiffusion process, vacancies should be created in the region between r_K (the Kirkendall radius) and r_{II} and

annihilated in the region r_I to r_K. Since few vacancy sinks are available at the nanolevel, porosity should in fact occur. Prasad and Paul showed that for a pure element core, porosity should occur only at interface *I* and a good nanotube will thus form from a nanorod.

A molecular dynamics (MD) simulation of the formation by diffusion of a hollow nanoparticle has not been performed. Such a simulation is likely to be computationally extremely time consuming because of the two requirements of a fairly large difference in mobility of the two atomic species in order to obtain observable porosity and a relatively long annealing time.

Kinetic Monte Carlo (KMC) calculations represent a computationally much more attractive alternative to molecular dynamics to demonstrate the formation of a hollow nanoparticle. However, it should be recognized that KMC calculations in general require at the outset the specification of a basic diffusion mechanism, e.g. the vacancy mechanism. This might not appear to be a problem since vacancies certainly provide the principal means for diffusion in bulk metals. However, it has been found in MD simulations that demonstrate the shrinkage of very small hollow Pd nanospheres (see further below) that vacancies do not in fact provide the only vehicles for atomic mobility: atoms have been found to move by means of moving Shockley partial dislocations that form at the surface of the nanosphere.

KMC calculations provide a useful means for visualizing the evolution of kinetics processes. Furthermore, the inter-site transition rates can be readily scaled to real time. KMC simulations of the formation (and shrinkage) of a hollow nanosphere have been performed very recently by the authors [28]. An Ising alloy model was employed where the nearest neighbour interactions between the atoms (A-A, B-B and A-B) were all set equal thus resulting in a random distribution of the atomic species.

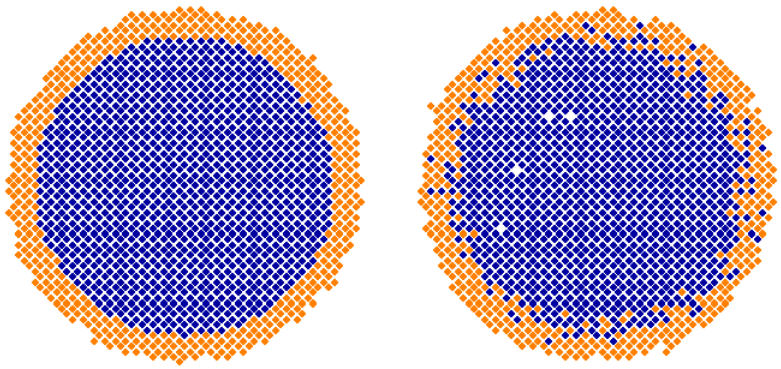

(a) (b)

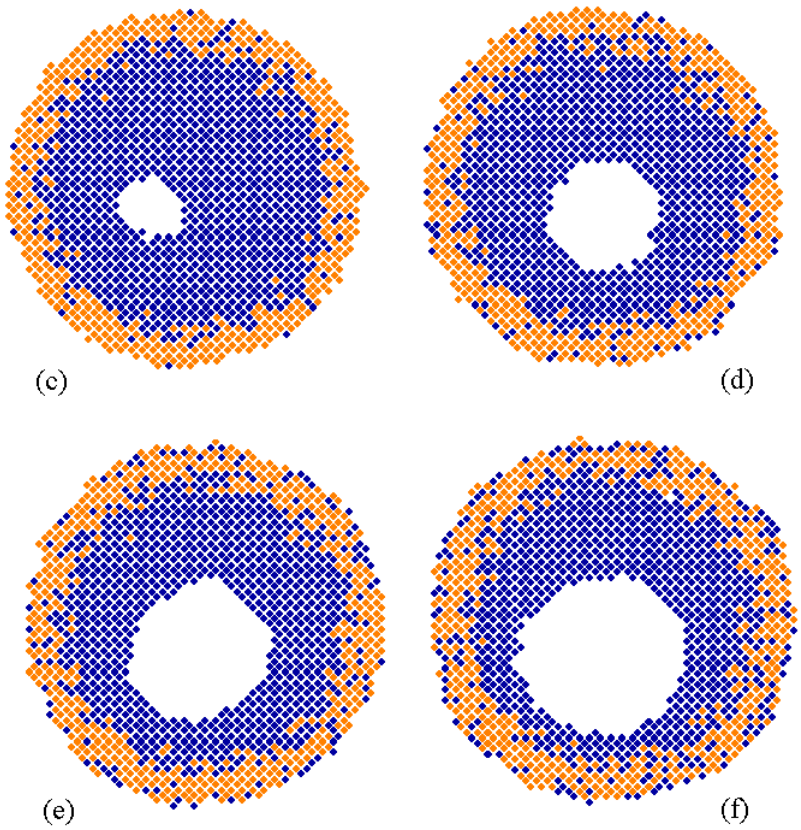

Fig. 1: Selected snapshots of the interdiffusion process in the initially A-core – B-shell nanoparticle model. Snapshots are taken at the beginning of the simulation (a) and after $\nu_{0A}t \approx 345955$ (b), $\nu_{0A}t \approx 449741$ (c), $\nu_{0A}t \approx 657314$ (d), $\nu_{0A}t \approx 864886$ (e), $\nu_{0A}t \approx 1349220$ (f) (ν_{0A} is the effective attempt frequency of A atoms for exchange with a vacancy). Only the same central cross-sections are shown [28].

However, the model is not the same as Manning's well known random alloy model [26] because there is both a small indirect attraction between neighbouring vacancies and a definable equilibrium vacancy composition. In the KMC study, the values of the interactions were adjusted so that the vacancy composition was close to a typical bulk value at diffusion temperatures $c_V^{eq} \sim 1.24 \times 10^{-4}$. In the simulation, the fast diffuser A (the core) was set to have an atom attempt frequency ν_{0A} three orders of magnitude larger than the slow diffuser B (the shell), ν_{0B}. The well-known 'Metropolis transition probability' was used in the calculations [29]. Although this transition probability is not particularly

realistic for a diffusion process, the number of Monte Carlo jump attempts scales transparently to real time.

In Fig. 1 a sequence of snapshots at various times for a system of 76,429 atoms is shown of the formation process of a hollow nanosphere of an alloy starting from two pure metals. The interdiffusion process has not gone to completion in this figure. There are no internal interfaces in this model: the core (A), the shell (B) and the formed alloy are all isomorphous. The structure contained no vacancies at the commencement of the simulation. During interdiffusion, vacancies form at the surface of this bimetallic nanosphere and diffuse into the interior via a small number of percolating paths of A through the shell of slow moving atoms (B). Once the vacancies reach the core they quickly mix with A atoms and lose connection to the percolating paths to the surface. Since there are no existing vacancy sinks, very considerable vacancy supersaturation now builds up in the core. This is clearly shown in Fig. 2 which shows the vacancy concentration in the core and the diffusion zone as a function of time. (In this figure $\varepsilon = r_{\mathrm{i}}/r_{\mathrm{e}}$, where r_{i} is the radius of the void and r_{e} is an external radius of the hollow nanosphere.) As time progresses, the vacancy composition in both the core and diffusion zone is seen to increase by about a factor of thirty (in this case) over the equilibrium vacancy composition value. The increase is greatest in the core region. The vacancies are in effect kinetically trapped in the core of the nanoparticle: they cannot return to the surface because there are insufficient number of paths to provide the means for long range diffusion to return there.

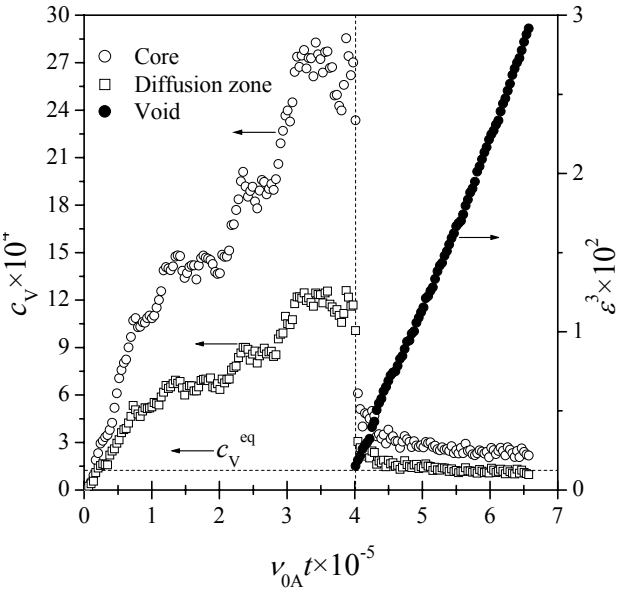

(a)

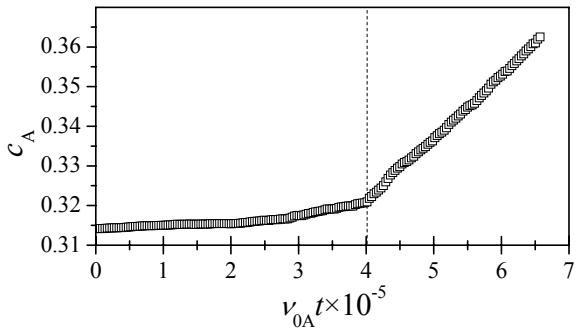

(b)

Figure 2. Time-dependencies of: (a) – the average vacancy compositions inside the core and diffusion zone of the nanoparticle model as well as the ratio ε^3 of the number of virtual lattice sites within the void to the total number of lattice sites inside the whole of the nanoparticle, and (b) – the average composition of A atoms inside the 'diffusion zone' (ν_{0A} is the effective attempt frequency of A atoms for exchange with a vacancy). The horizontal dashed line shows the equilibrium vacancy composition c_V^{eq} for this model. The vertical dashed line indicates the time at which the void appears to form [28].

Supersaturation of the vacancies inside the core results in a steep vacancy composition gradient in the diffusion zone and in fact, as they enter from the surface the vacancies actually diffuse uphill i.e. against their concentration gradient. The increase of the vacancy composition gradient is seen to restrict the out-flux of A atoms into the shell and hence tends to suppress the interdiffusion process. After a certain gestation time, the vacancies nucleate into a large void that forms roughly in the centre of the nanoparticle. The vacancy composition everywhere in the core and diffusion zone collapses, essentially down to the equilibrium vacancy composition level.

It is also seen in the same figure that at the same time, the average concentration of A in the diffusion zone now increases significantly as the vacancy in-flux now suddenly increases the rate of mixing of A and B.

3. Shrinkage of Hollow Nanoparticles

It was noted in [23] that hollow nanospheres should be unstable in principle and, with time, will have a tendency to shrink into a solid nanosphere. This is because the resulting reduction in surface area should be more advantageous from an energy reduction point of view: $\gamma\left(r_i^2 + r_e^2\right) > \gamma\, r_f^2$ (γ is the surface energy, r_i and r_e are the inner and external radii of a hollow nanosphere, r_f is the radius of a collapsed compact nanosphere). Shrinkage of hollow nanoparticles has recently been observed in the case of Cu_2O [5]. A considerable body of theoretical work and computer simulations has been published that explores the shrinkage phenomenon. In accordance with [23] the mechanism of shrinking can be considered as a result of the vacancy flux going from the

inner surface to the outer surface. The driving force for such a flux is the difference between the vacancy concentrations c_V on the inner and external surfaces.

This physical picture of the shrinking of hollow nano-objects seems reasonable if we make the assumption that the equilibrium vacancy composition c_V^{eq} in the bulk of the system does not differ strongly from the equilibrium vacancy composition near a planar surface ($c_V^{eq} \approx c_V^0$) or if $c_V^{eq} < c_V^0$, and either the external radius is much larger than the inner radius (so we can consider such a hollow nano-object as an infinite bulk system with a spherical void inside) or conversely, that the nanoshell is so thin, that the equilibrium vacancy composition c_V^{eq} in the bulk is unreachable.

Starting with a one component hollow nanosphere, Gusak and colleagues [30] employed Gibbs-Thomson type expressions for the vacancy compositions at the inner and outer curved surfaces. For a hollow nanosphere (and nanotube) with internal radius r_i and external radius r_e, the variation of vacancy composition near the surfaces with the number of vacancies in the void N_V^{void} is given by the Gibbs-Thomson equation:

$$c_V^{\pm} = c_V^{eq} \exp\left(\pm \frac{\partial \Delta G_S / \partial N_V^{void}}{kT} \right), \tag{3}$$

$\Delta G_S = \gamma S$ is the free energy of the spherical surface with a principal radius of curvature r ($r = r_i$ or $r = r_e$) and S is the surface area. In the above formula, the curvature is taken as positive for the inner surface and negative for the external surface. Since for a spherical geometry, we have that:

$$\frac{\partial \Delta G_S}{\partial N_V^{void}} = \frac{\partial \Delta G_S}{\partial r} \frac{\partial r}{\partial N_V^{void}} = \frac{2\gamma\Omega}{r}, \tag{4}$$

Eq. 3 reduces to:

$$c_V^{\pm} = c_V^{eq} \exp\left(\frac{\beta}{\pm r} \right), \tag{5}$$

where $\beta = 2\gamma\Omega / kT$ for a hollow nanosphere and Ω is the atomic volume. Assuming steady state for the vacancy composition and a linear approximation of the Gibbs-Thomson equation, Gusak et al. [30] found a numerical solution for the collapse time of a hollow nanosphere by diffusion. Using the same model, Evteev et al. [31] later derived exact solutions for the collapse time for both one component hollow nanospheres and nanotubes. KMC calculations have verified their expressions [32].

MD simulation has been used to study defect formation and distribution in a hollow Pd nanosphere (76,657 atoms) as well as its stability/shrinkage behaviour [33]. Interestingly, it was shown that at 1500 K, which is apparently very close to the melting point of the simulation system, the hollow Pd nanosphere does not actually shrink until it is completely melted. The melting starts from the outside surface.

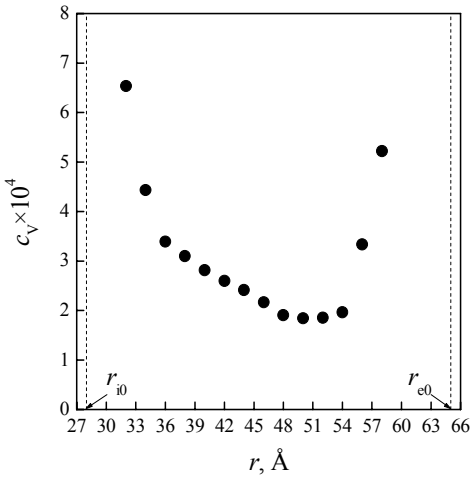

Fig. 3: MD simulation of the distribution of vacancies within a *Pd* hollow nanosphere at 1450 K [33].

At 50 degrees below the melting point the results of MD simulation unequivocally demonstrate that the vacancy composition profile across the nanoshell then develops a minimum [33], see Fig. 3. These results are consistent with the idea that the free energy of vacancy formation with respect to a planar surface in a crystal depends on the distance from the surface because of surface and subsurface relaxation, with the result that $\Delta g_{\mathrm{f}}^{0} + 2\gamma\Omega/r_{\mathrm{e}} < \Delta g_{\mathrm{f}}^{\mathrm{eq}}$. Furthermore, surface and subsurface relaxation processes can influence (in varying degrees) the relative changes of vacancy formation free energies $\Delta g_{\mathrm{f}}^{\mathrm{i}}$, $\Delta g_{\mathrm{f}}^{\mathrm{e}}$ and $\Delta g_{\mathrm{f}}^{0}$ because of the difference in sign and value of the curvature of the surfaces. Indeed, because of surface and subsurface relaxation processes, it can be supposed that the largest relative decrease being to $\Delta g_{\mathrm{f}}^{\mathrm{e}}$ (a negative curvature surface has the highest surface free energy) followed by $\Delta g_{\mathrm{f}}^{0}$ and $\Delta g_{\mathrm{f}}^{\mathrm{i}}$. Thus, unlike a simple treatment (Eq. 5), we can expect that $c_{\mathrm{V}}^{\mathrm{i}} > c_{\mathrm{V}}^{\mathrm{eq}} < c_{\mathrm{V}}^{\mathrm{e}}$. In other words, a vacancy composition profile across a hollow nanoshell can then have a minimum and a hollow nanosphere should actually be in a state corresponding to a local minimum of the free energy. Accordingly, the growing of the vacancy composition in the shell should result in the increasing of the free energy of such a system, namely to an increase of the free energy part responsible for the volume of the nanoshell. Thus, a free energy barrier should obstruct the transition of the hollow nanosphere (by the vacancy mechanism) to a state corresponding to the global minimum of the free energy (shrinkage to a solid nanosphere).

The MD results were obtained just below the melting temperature, where one should expect the most extensive surface and subsurface relaxation. Unfortunately, at present it is impossible to determine on a MD simulation time-scale the vacancy composition profile inside a nanoshell at more moderate temperatures. Furthermore, the vacancy

formation free energy near a surface in an alloy should be a function of atomic composition because of surface and subsurface segregation phenomena. Moreover, for different kinds of hollow nanospheres (pure element, alloy, compound) with various types of atomic bonds (metallic, covalent, ionic) the vacancy composition profile across the nanoshell might well have a different shape.

The MD simulations also showed that besides vacancies, which formed on both surfaces of the hollow nanosphere, other defects such as Shockley partial dislocations, twins and stacking faults nucleated on the external surface as a result of its significant reconstruction. The density of the defects on the external surface increased with reduction of nanoshell size. It was shown that for very small hollow nanospheres a Shockley partial dislocation can transport material from the external surface to the inner one and lead to its shrinking. It is certainly conceivable that such mechanisms can account principally for the shrinkage of small hollow nanospheres without the participation of point defects such as vacancies.

The case of the shrinkage of a binary alloy nanoshell has also been investigated and is rather more complicated. The vacancy flux from inner to external surface, caused by the Gibbs-Thomson effect, leads to inward atomic fluxes of the atomic components of the binary alloy [30,34]. If diffusion of one species, for example A, proceeds faster, then A will segregate near the inner surface (another example of the Inverse Kirkendall effect). The resulting composition gradient of A will reduce the vacancy flux and hence will generate a tendency to suppress the shrinking process [30,34]. In a phenomenological analysis, Gusak and colleagues [30] showed that the shrinkage rate of a hollow binary nanosphere will be controlled by the diffusion of the slower species.

Evteev and colleagues [34] considered diffusion via vacancies in a hollow binary AB alloy nanosphere under the Gibbs-Thomson effect. They made use of the Onsager flux equations for the situation where there are no sources and sinks for vacancies. They found that the controlling parameter D of vacancy motion within a binary alloy nanoshell (or shrinking rate) can be written in the form:

$$D = \frac{\Omega kT}{c_{\mathrm{V}}} \frac{L_{\mathrm{AA}}L_{\mathrm{BB}} - L_{\mathrm{AB}}^2}{\left(c_{\mathrm{A}}L_{\mathrm{BB}} - c_{\mathrm{B}}L_{\mathrm{AB}}\right)\dfrac{J_{\mathrm{A}}}{J_{\mathrm{A}} + J_{\mathrm{B}}} + \left(c_{\mathrm{B}}L_{\mathrm{AA}} - c_{\mathrm{A}}L_{\mathrm{AB}}\right)\dfrac{J_{\mathrm{B}}}{J_{\mathrm{A}} + J_{\mathrm{B}}}} \varphi_{\mathrm{V}}, \quad (6)$$

where L_{AA}, L_{BB} and L_{AB} are the phenomenological coefficients, c_{A}, c_{B} and c_{V} are the compositions of species A, B and vacancies respectively, J_A and J_B are the atomic fluxes and

$$\varphi_{\mathrm{V}} = 1 + \frac{c_{\mathrm{V}}}{kT} \frac{\left(\partial \Delta g_{\mathrm{f}}/\partial r\right) + \left(\partial \Delta g_{\mathrm{f}}/\partial c_{\mathrm{A}}\right)\left(\partial c_{\mathrm{A}}/\partial r\right)}{\left(\partial c_{\mathrm{V}}/\partial r\right)} \quad (7)$$

can be regarded as the vacancy thermodynamic factor. This factor should arise if the vacancy formation free energy depends either on the distance from a surface due to subsurface relaxation or on atomic composition due to surface and subsurface segregation

phenomena, or both. Accordingly, the vacancy thermodynamic factor may well be important for the analysis of diffusion by vacancies inside a nano-object because in such a system, the fractions of subsurface and bulk atoms are of comparable magnitude. If it is assumed however that the vacancy thermodynamic factor is close to unity $\varphi_{\mathrm{V}} \approx 1$, then a steady-state approximation for vacancies should be quite reasonable. A range for the collapse time of a hollow binary alloy nanosphere can then be estimated by making use of the Moleko et al. [35] diffusion kinetics theory:

$$\left(c_{\mathrm{V}}^{\mathrm{eq}} D_{\mathrm{V}}\right)^{-1} < \frac{12\gamma\Omega t_{\mathrm{c}}}{kTr_{\mathrm{f}}^{3}\tau_{\mathrm{c}}} < \left(c_{\mathrm{V}}^{\mathrm{eq}} D^{(\mathrm{SS})}\right)^{-1}. \tag{8}$$

where D_{V} is the diffusion coefficient of the vacancies and $D^{(\mathrm{SS})}$ is a controlling parameter for shrinkage at steady state:

$$D^{(\mathrm{SS})} = \frac{\Omega kT}{c_{\mathrm{V}}} \frac{L_{\mathrm{AA}}L_{\mathrm{BB}} - L_{\mathrm{AB}}^{2}}{\left(c_{\mathrm{A}}L_{\mathrm{BB}} - c_{\mathrm{B}}L_{\mathrm{AB}}\right)\dfrac{c_{\mathrm{A}}}{c_{\mathrm{A}}+c_{\mathrm{B}}} + \left(c_{\mathrm{B}}L_{\mathrm{AA}} - c_{\mathrm{A}}L_{\mathrm{AB}}\right)\dfrac{c_{\mathrm{B}}}{c_{\mathrm{A}}+c_{\mathrm{B}}}}, \tag{9}$$

and

$$\tau_{\mathrm{c}} \approx \ln\left[\frac{\left(1-\varepsilon_0\right)\left(1+\varepsilon_0\right)^{3}}{\left(1-\varepsilon_0^{3}\right)^{\frac{4}{3}}}\right] - 2\varepsilon_0\frac{1-\varepsilon_0}{1-\varepsilon_0^{3}}, \quad \varepsilon_0 = \frac{r_{\mathrm{i}0}}{r_{\mathrm{e}0}}.$$

KMC calculations have been performed on an initially homogeneous equi-atomic hollow nanosphere using a model identical with that described above for the formation of a hollow nanosphere [34]. It was found that the faster moving species (A) segregates near the inner surface (the Inverse Kirkendall effect). The appearance of a composition gradient of the component A reduces the vacancy flux and hence generates a tendency to suppress the shrinking process as had been noted earlier [30]. At the same time, the increase of the collapse time of the KMC model of the hollow binary alloy nanosphere with increasing ratio of the jump frequencies is much smaller than could be expected at the steady-state approximation for atomic components. It was found that the collapse time of the KMC model of the hollow random binary alloy nanosphere is much less than the time required for obtaining steady-state conditions for the atomic components.

Preliminary ‘whole-of-life’ KMC simulations have also been carried out for a relatively small system (16,757 atoms) by the present authors.

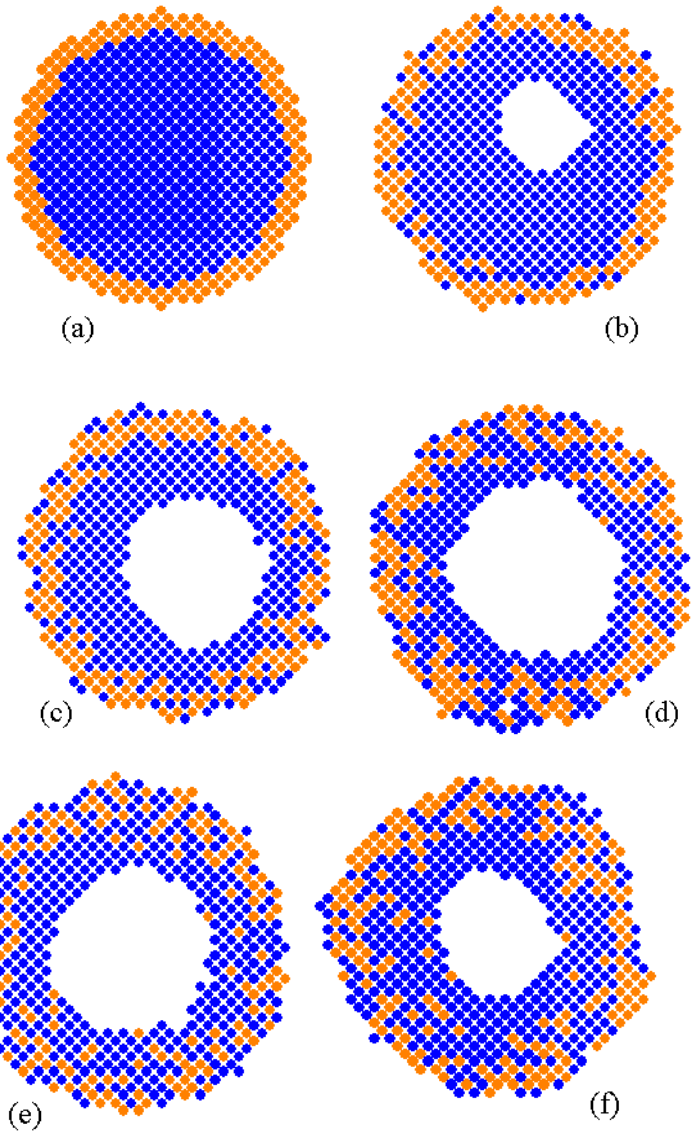
(a)
(b)
(c)
(d)
(e)
(f)

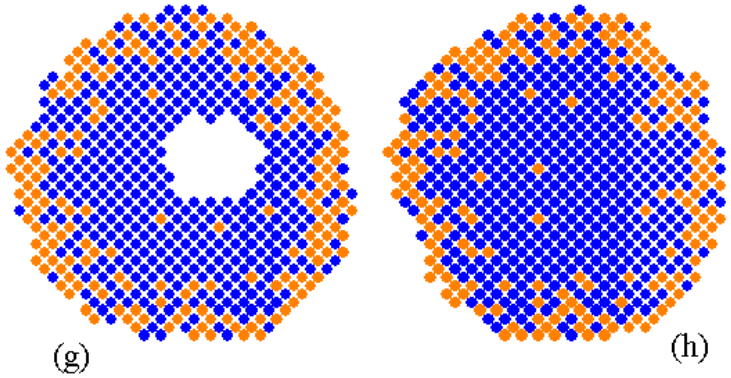

Fig. 4: Selected snapshots of the 'whole-of-life' interdiffusion process in the initially A-core – B-shell nanoparticle model. Snapshots are taken at the initial time of the simulation (a), after about 2.5% of the final time (b), after about 5% of the final time (c), after about 30% of the final time (maximum volume of the pore was observed at this time) (d), after about 55% of the final time (e), after about 90% of the final time (f), after about 99.9% of the final time (g), at the final time (h).

These simulations start from the initial bi-metallic configuration of Figure 1a (the system size used however was smaller than that used for Figure 1 as a concession to computational time). The simulation proceeds to the formation of the hollow nanosphere as described above in conjunction with Figure 1 and then proceeds further to the final subsequent shrinkage to a solid alloy nanosphere. The time evolution is shown in the sequence of snapshots in Figure 4. At least two important observations can be made from these preliminary 'whole-of-life' KMC simulations. First, it can be seen in Figure 4 d,e that the shrinkage stage actually starts before complete intermixing has been reached. Second, the shrinkage time is only about three times larger than the formation time (see Figure 5). This result does not support the theoretical prediction of Gusak and colleagues [30] that the shrinkage is a steady-state process and is controlled by the slower diffusing species (we recall that in this KMC model the fast diffuser A was set to have a atom-vacancy exchange rate three orders of magnitude larger than the slow diffuser B).

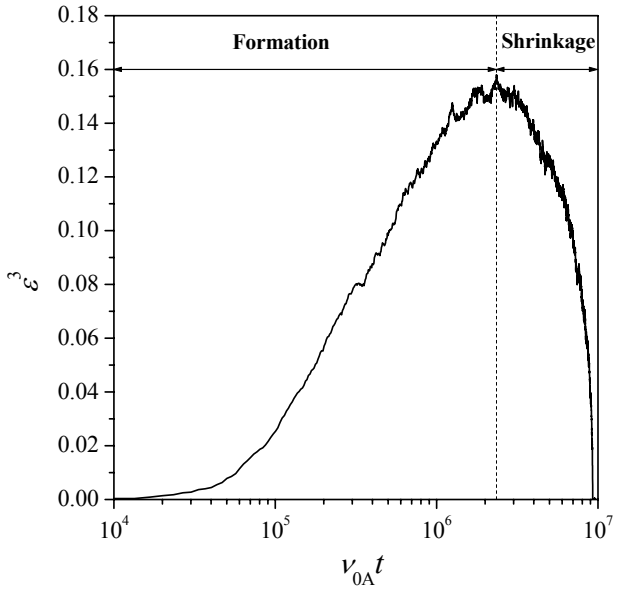

Fig. 5: Time-dependence of the void volume relative to the total volume of the sphere (ν_{0A} is the effective attempt frequency of A atoms for exchange with a vacancy; $\varepsilon=r_i/r_e$, where r_i is the radius of the void and r_e is an external radius of the hollow nanosphere).

4. Interdiffusion in Bimetallic Nanoparticles

Here, we discuss two rather extreme cases of interdiffusion in bi-metallic nanoparticles, both of which lead to segregation. In the first case (*Ag*-*Ni*) in the bulk, the two metals are almost immiscible. In the second case (*Pd*-*Ni*) in the bulk, the two metals show complete miscibility. It should also be noted that *Ni* has a much higher surface energy than *Ag* and *Pd*.

Interdiffusion in a Ag-Ni Bi-Metallic Nanoparticle

Interdiffusion was simulated by the MD method starting with a diffusion couple consisting of a core of *Ag* (959 atoms) covered by a shell of *Ni* (2,504 atoms) [36]. Since *Ni* has a much higher surface energy than *Ag* , it might be expected that it would be energetically advantageous for some *Ag* atoms to reside at the surface. Representative snapshots from the MD simulation during isothermal annealing at T = 950 K are shown in Fig. 6. It can be seen that *Ag* atoms diffuse quite rapidly through the *Ni*-shell and begin to accumulate on the surface of the nanosphere. The first *Ag* atoms that arrive at the surface of the nanosphere reside preferentially at edges, vertices and at sites at high energy faces. The later *Ag* atoms that come to the surface of the nanoparticle meet the previous *Ag* atoms on the surface and form small clusters there. However, this interdiffusion rate soon becomes very slow and almost stops when the average number of nearest *Ag* neighbours of the *Ag* atoms on the surface reaches two.

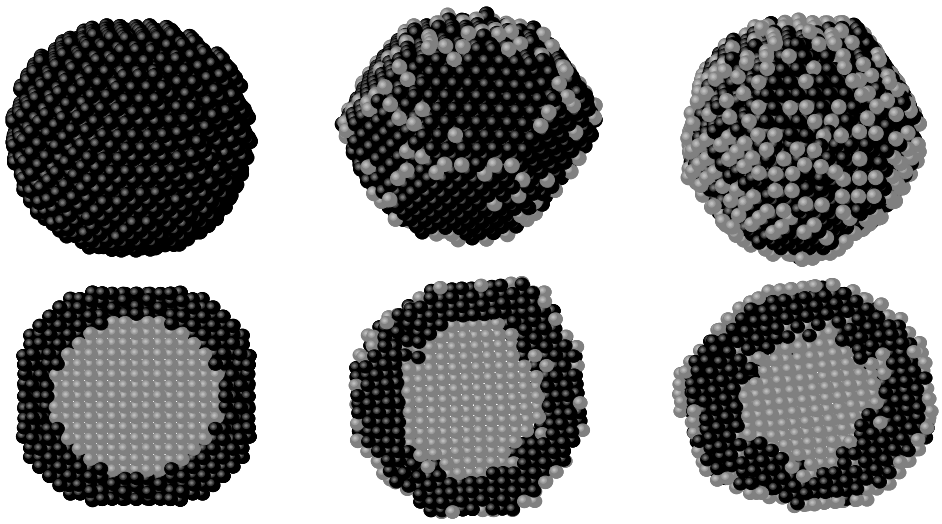

Fig. 6: Selected snapshots (after static relaxation) of the interdiffusion of a *Ag*-core – *Ni*-shell nanoparticle during annealing at $T = 950$ K. Snapshots are taken at the beginning of the simulation (a) and after ~ 0.03 μ s (b) and ~ 0.3 μ s (c). The surface and a central cross-section of the nanoparticle are shown in the top and bottom rows, respectively. *Ag* and *Ni* atoms are represented in gray and black, respectively.

Thus, the *Ag* atoms coming from the core to the surface by diffusion through the *Ni*-shell form a quite dispersed single surface layer. On the other hand, a well-defined *Ag* core still remains to occupy the centre of the nanosphere. Shown in Fig. 7(b) the atomic radial distribution of the *Ag* and *Ni* atoms illustrates the separation of the structure into a *Ag*-core – *Ni*-intermediate shell – *Ag*-dispersed surface sub-monolayer. It can be seen in Fig. 7(b) that only few *Ag* atoms exist in the intermediate shell of the nanosphere.

These results agree well with an earlier MD simulation of the growth of *Ag*-*Ni* nanospheres by deposition of *Ni* atoms onto a *Ag* core [37], where the final number of atoms in the system was ~ 400, which is one order of magnitude less. Thus, it is evident that the phenomenon of segregation of *Ag* to form a *Ag*-*Ni*-*Ag* surface–sandwich structure in *Ag*-*Ni* nanoparticles is quite general and apparently does not have a strong dependence on size.

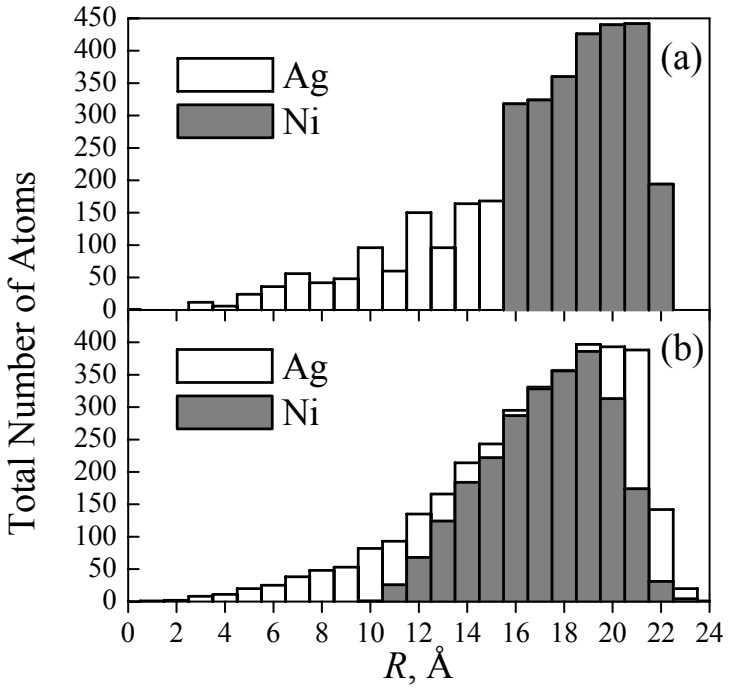

Fig. 7: Atomic radial distribution in the *Ag-Ni* nanosphere model at the initial time (a) and after the annealing at $T = 950$ K during ~ 0.3 μs (b).

Interdiffusion in a Pd-Ni Bi-Metallic Nanoparticle

In the *Pd-Ni* system, in complete contrast with the *Ag-Ni* system, there is complete miscibility in the bulk. MD simulations of interdiffusion in the bi-metallic nanoparticle were performed starting from a core of *Ni* (1088 atoms) surrounded by a shell of *Pd* (2132 atoms) [36, 38, 39]. During the first ~ 0.03 μ s of MD annealing at 1000 K, the distorted crystal order of the nanoparticle starts to be broken at the interface between the core and shell rather quickly. Then the structure of the whole nanoparticle evolves by interdiffusion to a disordered *Pd*-rich solid solution. Monitoring of the structure of the nanoparticle by Voronoi polyhedron analysis shows a significant increase of icosahedral short-range ordering during the next stage of annealing up to ~ 0.5 μ s. The centres of the icosahedral cages are almost always the smaller *Ni* atoms, surrounded by four *Ni* and eight *Pd* atoms (see Fig. 8). The most favourable sites for *Ni* icosahedra are in the subsurface shell. Indeed, after ~ 0.5 μ s of the annealing, among the 790 Ni atoms that have gone from the initial core to the shell, the icosahedra fraction is ~ 78 % whilst ~ 52 % of the 298 *Ni* atoms remain in the core (see Figs. 9 and 10b).

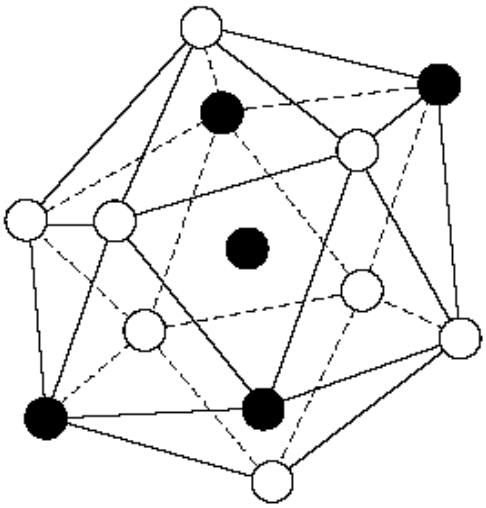

Fig. 8: The most preferred icosahedral environment of *Ni* atoms in the *Pd-Ni* nanoparticle model: four *Ni* and eight *Pd* nearest neighbours (Ni is black, Pd is white).

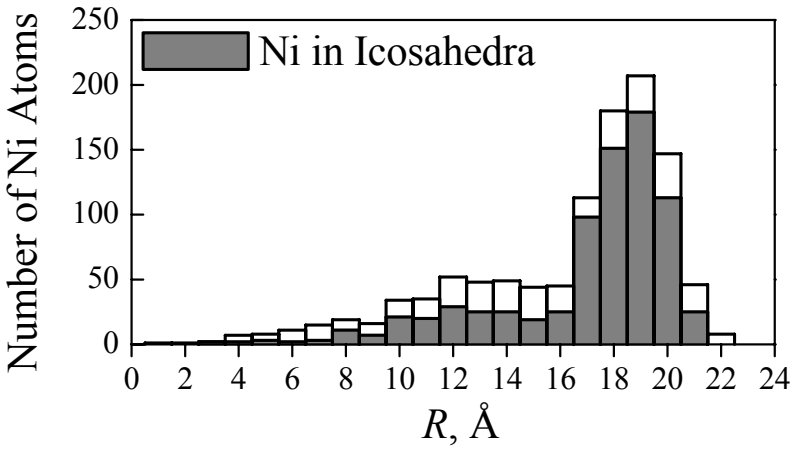

Fig. 9: Radial distribution of *Ni* atoms having an icosahedron as a coordination polyhedron in the *Pd-Ni* nanoparticle model after annealing at $T = 1000$ K for ~ 0.5 μ s.

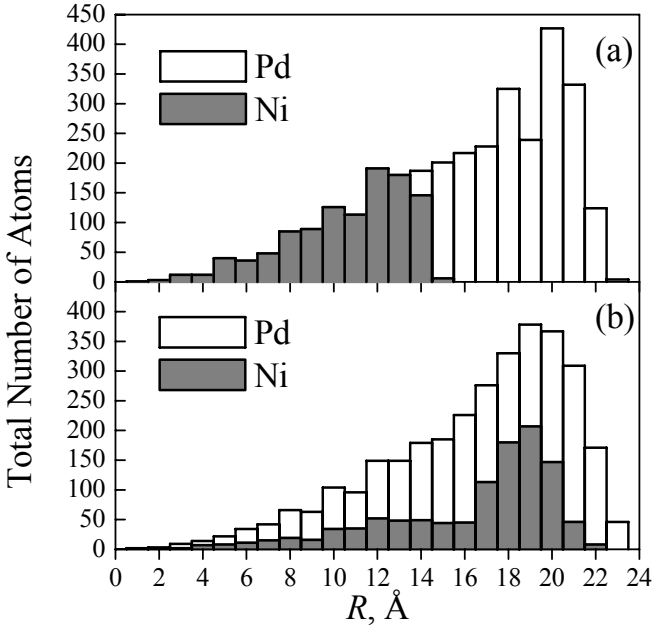

Fig. 10: Atomic radial distribution in the *Pd*-*Ni* nanoparticle model a) at the initial time and b) after the annealing at T = 1000 K for ~ 0.5 μ s.

It was established that *Ni* atoms coming by way of interdiffusion to the shell begin to accumulate in a layer just below the surface, and then locate themselves in the centres of interpenetrating icosahedra in order to generate a subsurface layer (shell) as a Kagomé net (see Fig. 11a), which is almost completely covered by *Pd* atoms on both sides. Planar layers of Kagomé nets are the basic structure of the well-known bulk Frank-Kasper phases of certain intermetallic alloys [40]. This subsurface Kagomé net shell of Ni atoms efficiently allows the minimization of the nanoparticle surface energy by increase of the average number of nearest neighbours of *Pd* surface atoms in comparison with the close-packed f.c.c. (111) surface. Indeed, the Kagomé net layer (*K*) of *Ni* is covered from each side by two *Pd* layers (*A′* and *A″*), which can be obtained by splitting of a layer *A* – close packed f.c.c. (111) layer (see Fig. 11b). The formation of such a five-layer *A′A″KA″A′* surface structure results in a third of the surface *Pd* atoms having increased their number of nearest neighbours from 9 (the close packed f.c.c. (111) surface) to 13. The number of *Pd* atoms in each couple layers *A′* and *A″* coincides with the number of *Ni* atoms in the Kagomé net layer, therefore, the total atomic fraction involved in the build up of the five-layer *A′A″KA″A′* Pd_2Ni ordering surface–sandwich structure in the nanoparticle with consideration of some imperfection of icosahedral order in Kagomé net layer estimated at ~ 70 %. Thus, only ~ 30 % atoms are located in the core of nanoparticle and form there a non-crystalline *Pd*-rich solid solution with quite strongly developed icosahedral short-range order. This final arrangement of the nanoparticle is the result of competition

between the shell (~ 70 % atoms) and the core (~ 30 % atoms) contributions to the excess energy.

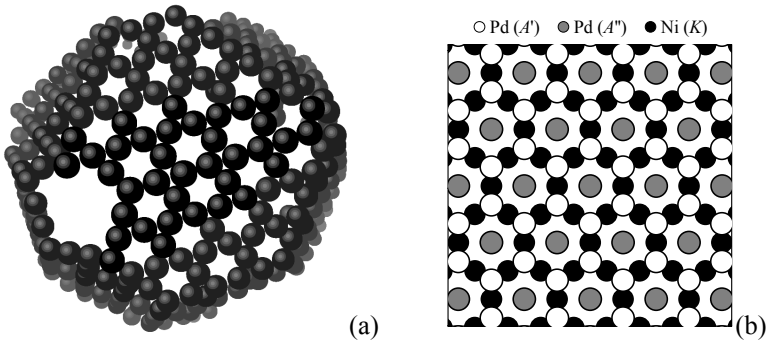

Fig. 11: a) – Snapshot of the *Ni* subsurface shell having a structure of the Kagomé net with 'sequence faults' after ~ 0.3 μs of annealing at T = 1000 K. The great majority of *Ni* atoms of the subsurface shell are located in the centres of interpenetrating icosahedra and have four *Ni* and eight *Pd* nearest neighbours. For clarity, only a half of the shell and only *Ni* atoms at centres of icosahedra are shown on the perspective projection with size and grey-scale graduation. b) – Illustration of atomic positions of *Pd* and *Ni* atoms on a perfect fragment of surface structure *A′A″KA″A′*. Layers *A′* and *A″* of *Pd* can be obtained by splitting of a layer *A* – close packed f.c.c. (111) layer; layer *K* of *Ni* is a Kagomé net layer.

Thus, the MD experiments demonstrate that under certain conditions diffusion mediated segregation phenomena at the nanoscale can be observed in systems with completely different phase diagrams in the bulk. For the *Ag-Ni* system, where the miscibility is very low, it is seen that Ag partially segregates to the surface, ostensibly to lower the surface energy associated with *Ni*. For the *Ni-Pd* system, where miscibility in the bulk is complete, at the nano-scale, a new type of chemical ordering unknown in the bulk can occur.

Acknowledgement
We acknowledge research support from the Australian Research Council.

[1] Y. Yin, R.M. Rioux, C.K. Erdonmez, S. Hughes, G.A. Somorjai and A.P. Alivisatos, Science Vol. 304 (2004), p. 711.
[2] A.D. Smigelskas and E.O. Kirkendall, Trans AIME, Vol. 171 (1947), p. 130
[3] C.M. Wang, D.R. Baer, L.E. Thomas, J.E. Amonette, J. Antony, Y. Qiang and G. Duscher, J. Appl. Phys., Vol. 98 (2005), p.94308.
[4] C. Han, X. Wu, Y. Lin, G. Gu, X. Fu and Z. Hi, J. Mater. Sci., Vol. 41 (2006), p. 3679.
[5] R. Nakamura, D. Tokozakura and H. Nakajima, J. Appl. Phys., Vol. 101 (2007), p. 074303.
[6] R. Nakamura, J-G Lee, D. Tokozakura, H. Mori and H. Nakajima, Materials Letters, Vol. 61 (2007), p.1060

[7] R. Nakamura, J-G Lee, D. Tokozakura, H. Mori and H. Nakajima, Phil. Mag., Vol. 88 (2008), p. 257.
[8] L. Xie, J. Zhang, Y. Liu, Y. Li and X. Li, Chem. Mater, Vol. 20 (2008), p282-286.
[9] C.H. Ng, H. Tan and W.Y. Fan, Langmuir, Vol. 22 (2006), p. 9712.
[10] J. Gao, B. Zhang, X. Zhang and B. Xu, Angew. Chem. Int. Ed., Vol. 45 (2006), p. 1220.
[11] Q. Li and R. M. Penner, Nano Lett., Vol. 5 (2005), p. 1720.
[12] H.J. Fan, M. Knez, R. Scholz, K. Nielsch, E. Pippel, D. Hesse, M. Zacharias and U. Gösele, Nature Mater., Vol. 5 (2006), p. 627.
[13] F. Aldinger, Acta Met., Vol 22 (1974), p.923.
[14] Y.E. Geguzin, Why and how vacancies disappear, Science Publishers, Moscow,1976.
[15] N. Toshima, M. Kanemaru, Y. Shiraishi and Y. Koga, J. Phys. Chem. B Vol. 109 (2005), p. 16326.
[16] S. Takenaka, Y. Shigeta, E. Tanabe and K. Otsuka, J. Phys. Chem. Vol. 108 (2004), p.7656.
[17] S. Sao-Joao, S. Giorgio, J.M. Penisson, C. Chapon et al., J. Phys. Chem. Vol. 109 (2005), p.342.
[18] A.B. Hungría, J.J. Calvino, J.A. Anderson and A. Martínez-Arias, Appl. Catal. Vol. 62 (2006), p.359.
[19] P. Miegge, J.L. Rousset, B. Tardy, J. Massardier et al., J. Catal. Vol. 149 (1994), p.404.
[20] P. Herman, J.M. Guigner, B. Tardy, Y.Jugnet et al., J. Catal. Vol. 163 (1996), p. 169.
[21] A.C. Michel, L. Lianos, J.L. Rousset, P. Delichère et al., Surf. Sci. Vol. 416 (1998), p.288.
[22] L. Porte, M. Phaner-Goutorbe, J.M. Guigner, J.C. Bertolini: Surf. Sci. Vol. 424 (1999), p.262.
[23] K.N. Tu and U. Gösele: Appl. Phys. Lett., Vol. 86 (2005), p.093111.
[24] I.V. Belova and G.E. Murch, J. Phase Equil. and Diffus., Vol. 26 (2005), p.430.
[25] J. Philibert, Atom Movements: Diffusion and Mass Transport in Solids, Editions de Physique, les Ulis, 1991.
[26] J.R. Manning, Diffusion Kinetics for Atoms in Crystals, Van Nostrand Reinhold, Princeton 1968.
[27] S. Prasad and A. Paul, Appl. Phys. Lett., Vol. 90 (2004), p. 233114.
[28] A.V. Evteev, E.V. Levchenko, I.V. Belova and G.E. Murch, J Nano Research, accepted and in press.
[29] N. Metropolis, A.W. Rosenbluth, M.N. Rosenbluth, A.H. Teller and E. Teller, J. Chem. Phys., Vol. 21 (1953), p.1087.
[30] A.M. Gusak, T.V. Zaporozhets, K.N. Tu and U. Gösele, Phil. Mag., Vol. 85 (2005), p. 4445.
[31] A.V. Evteev, E.V. Levchenko, I.V. Belova and G.E. Murch, Phil. Mag., Vol. 87 (2007), p 3787.
[32] A.V. Evteev, E.V. Levchenko, I.V. Belova and G.E. Murch, Def. Diff. Forum, Vol. 277 (2008), p. 21.

[33] A.V. Evteev, E.V. Levchenko, I.V. Belova and G.E. Murch, Sol. St. Phen., Vol. 129 (2007), p.125.
[34] A.V. Evteev, E.V. Levchenko, I.V. Belova and G.E. Murch, Phil. Mag., Vol. 88 (2008), p 1524-1541.
[35] L.K. Moleko, A.R. Allnatt and E.L. Allnatt, Phil. Mag. A, Vol. 59 (1989), p. 141.
[36] E.V. Levchenko, A.V. Evteev, I.V. Belova and G.E. Murch, Def. Diff. Forum, in press
[37] F. Baletto, C. Mottet and R. Ferrando: Phys. Rev. Lett. Vol. 90 (2003), p. 135504.
[38] A.V. Evteev, E.V. Levchenko, I.V. Belova and G.E. Murch, Def. Diff. Forum, Vol. 277 (2008), p. 207.
[39] A.V. Evteev, E.V. Levchenko, I.V. Belova and G.E. Murch, Phys. Chem. Chem. Phys., (2009), DOI: 10.1039/b822112j.
[40] F.C. Frank and J.S. Kasper, Acta Cryst., Vol. 11 (1958), p. 184; Vol. 12 (1959), p. 483.